Liquid Crystals
Publication details, including instructions for authors and subscription information:
http://www.informaworld.com/smpp/title~content=t713926090

High-resolution calorimetric investigation of the existence of a nematic phase for the dodecylcyanobiphenyl liquid crystal

George Cordoyiannis[a]; Zdravko Kutnjak[b]; Gojmir Lahajnar[b]; Christ Glorieux[a]; Jan Thoen[a]
[a] Departement Natuurkunde en Sterrenkunde, Katholieke Universiteit Leuven, Laboratorium voor Akoestiek en Thermische Fysica, Leuven, Belgium [b] Condensed Matter Physics Department, Institute Jožef Stefan, Ljubljana, Slovenia

To cite this Article Cordoyiannis, George , Kutnjak, Zdravko , Lahajnar, Gojmir , Glorieux, Christ and Thoen, Jan(2009) 'High-resolution calorimetric investigation of the existence of a nematic phase for the dodecylcyanobiphenyl liquid crystal', Liquid Crystals, 36: 3, 231 — 237
To link to this Article: DOI: 10.1080/02678290902807324
URL: http://dx.doi.org/10.1080/02678290902807324

Liquid Crystals,
Vol. 36, No. 3, March 2009, 231–237

Taylor & Francis
Taylor & Francis Group

High-resolution calorimetric investigation of the existence of a nematic phase for the dodecylcyanobiphenyl liquid crystal

George Cordoyiannis[a], Zdravko Kutnjak[b], Gojmir Lahajnar[b], Christ Glorieux[a] and Jan Thoen[a]*

[a]*Laboratorium voor Akoestiek en Thermische Fysica, Departement Natuurkunde en Sterrenkunde, Katholieke Universiteit Leuven, Celestijnenlaan 200D, 3001 Leuven, Belgium;* [b]*Condensed Matter Physics Department, Institute Jožef Stefan, Jamova 39, 1001 Ljubljana, Slovenia*

(Received 6 November 2008; final form 9 February 2009)

We have employed high-resolution calorimetric techniques in order to investigate the unresolved issue of the existence of a nematic phase for the liquid crystal dodecylcyanobiphenyl. Various heating and cooling runs were performed on dodecylcyanobiphenyl samples of different origin and their analysis did not reveal any signature of a nematic phase. The calorimetric results are presented in detail and they are additionally supported by optical polarising microscopy observations.

Keywords: adiabatic scanning calorimetry; ac calorimetry; dodecylcyanobiphenyl; heat capacity

1. Introduction

The first homologues of the *n*-alcyl cyanobiphenyl family of liquid crystals (nCBs, $n = 5$–7) were synthesised more than 30 years ago (*1*). Their stability and excellent electro-optical properties close to room temperature (*2*) made them attractive materials for display technology. In the following years higher homologues ($n = 8$–14, according to our knowledge) of the same family were synthesised. Several compounds of the nCB series have been studied extensively using various techniques, such as differential scanning calorimetry (DSC), high-resolution calorimetry, light scattering, dielectric spectroscopy and X-rays (*3–8*), and phase diagrams have been constructed (*9*).

Nevertheless, there are still some issues that remain unresolved, such as the existence of a nematic phase for dodecylcyanobiphenyl (12CB). By means of adiabatic calorimetry performed in steps, Buleiko and Voronov (*10*) claimed that they observed a nematic (N) phase for the pure and confined 12CB. One may assume that porous-induced confinement enhances the nematic ordering and finally induces a N phase. Nevertheless, the finding that the pure 12CB also exhibits a N phase is very surprising, since it has not been found in other homologues higher than 9CB (*4, 6*). In one of the very first DSC studies a N phase was reported for 11CB (*3*), but subsequent high-resolution calorimetry and DSC studies (*4, 6*) showed that only one transition from the isotropic to the smectic A phase (I–SmA) occurs. Thus, we decided to resolve the elusive picture about 12CB by performing a systematic high-resolution calorimetric study.

The existence of a N phase for pure 12CB means that the N ordering is simply enhanced in case of confinement (*10*). For 12CB, in particular, the influence of surfaces on the growth of smectic ordering was reported almost 15 years ago by Iannacchione *et al.* (*11, 12*). It was systematically explored for thin 12CB samples placed in cells with different surface coating (*11*), as well as for samples confined in anopore membranes with surface agents of various chain lengths (*12*). In these measurements no indication for a N phase was found for 10CB or 12CB. The nonexistence of a N phase for the pure sample, implies that the N range which is clearly observed for 12CB trapped in a glass matrix (*10*), is apparently induced in the smectic liquid crystal due to the confinement.

2. Materials and methods

Aiming to arrive at a solid conclusion we looked for a set of different 12CB samples. Three different samples were used in this study, the first supplied by Merck (melted and solidified only once before), the second obtained by BDH around 1985 (always kept sealed in its package and opened for the first time for the current measurements), and a third recently synthesised at Likchem, Warsaw, Poland (with mentioned purity higher than 99.92%). For simplicity, we henceforth refer to the above samples with the acronyms A, B and C, respectively. Sequential heating and cooling runs were performed for A, B and C. After being mounted to the cells and prior to the measurements

*Corresponding author. Email: jan.thoen@fys.kuleuven.be

ISSN 0267-8292 print/ISSN 1366-5855 online

DOI: 10.1080/02678290902807324
http://www.informaworld.com

all samples were degassed and remained in the I phase for a few hours.

The initial measurements were performed on sample A in a computerised high-resolution ac-calorimeter (ACC), operated in both ac and relaxation modes. The ac mode is sensitive only to the continuous changes of the enthalpy, while the relaxation mode probes both continuous and discontinuous (i.e. latent heat, L) changes. Apart from the heat capacity C_p the temperature dependence of the phase ϕ is also recorded during an ac run, giving important information about the order of the transition. When a first-order (i.e. discontinuous) transition appears, the phase ϕ shows an anomalous behaviour indicative of the two-phase region. In that case an additional relaxation run is performed. By comparing the C_p anomalies of the ac and relaxation runs one can determine the latent heat. In the case of a second-order (i.e. continuous) transition ϕ behaves normally and the ac and relaxation runs yield identical C_p curves. A detailed description of the two modes of operation can be found elsewhere (*13, 14*).

For the ACC, heating and cooling measurements of sample A were performed using ac and relaxation modes. Its quantity was 38 mg and it was placed in homemade silver cells. A heater is mounted on one side of the cell to apply the power to the sample and a thermistor is placed on the other side to accurately measure the temperature. For ac runs the amplitude of the temperature oscillations at $\omega = 0.0767\ s^{-1}$ was 11 mK far away from the transition and 1.8–6 mK at the transition. The scanning rate was 100–150 mK per hour near the melting transition. For the relaxation runs steps of 0.5 K were used.

Heating and cooling runs on all samples (A, B and C) were carried out using high-resolution adiabatic scanning calorimetry (ASC). The ASC apparatus is also computer-controlled and it consists of four stages. For the current measurements the inner stage was a 22 g tantalum cell, that contained the 12CB. The space between the cell and the three surrounding shields is vacuum pumped. A detailed description of ASC can be found elsewhere (*15, 16*). Each run yields the temperature dependence of both the heat capacity C_p and the enthalpy H. ASC can easily distinguish between continuous and discontinuous transitions and allows very precise determination of the latent heat from the enthalpy curves. One important feature of this technique is that, in its principal modes of operation, it applies a constant heating or cooling power instead of a constant scanning rate. In the coexistence range of a first-order transition the scanning rate is substantially reduced, since the applied power is dissipated not only for the temperature change of the sample but also for the change between the two coexisting phases. This decrease of the rate results in excellent resolution data and accurate determination of the coexistence range and the latent heat values. Quantities of 0.55, 1.20 and 1.04 g were used for the ASC experiments of samples A, B and C, respectively.

3. Results and discussion

In this section the experimental results for all samples are discussed, starting with the ACC runs for A. In Figure 1 the heat capacity C_p is shown for sample A, upon cooling. As shown in the inset to Figure 1 there is only one broad coexistence range between the isotropic and the smectic A phase. No additional anomaly indicating the onset of the nematic phase was observed in the vicinity of this anomaly. About 3 K below the main isotropic to smectic A anomaly, another very small anomaly (indicated by an arrow in Figure 1) was detected. This tiny anomaly was reproducible, i.e. observed on both heating and cooling. However, subsequent optical polarising microscopy observations have ruled out the possibility that this small anomaly could be related to the formation of the nematic phase. Namely, the formation of focal-conic smectic domains took place exactly at the temperature of the large C_p anomaly at 331.1 K (within the few millikelvin error due to different thermometry at the optical microscopy sample holder). At the temperature of the small C_p anomaly only very little change in the size of the smectic focal-conic domains took place, probably related to the elastic annealing of domain wall pinning due to the presence of a very small concentration of impurities. We do not believe that this

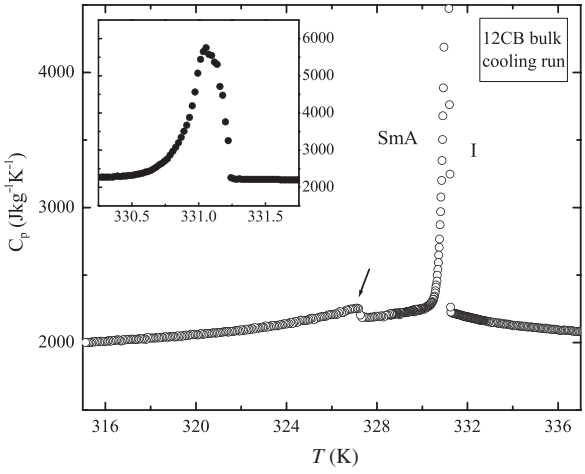

Figure 1. The $C_p(T)$ of sample A obtained in an ACC cooling run. The inset shows in detail the C_p anomaly related to the I–SmA phase transition. The arrow points to the small C_p anomaly that was observed (on both heating and cooling) at about 3 K lower than the I–SmA transition.

very small anomaly is related to surface effects similar to those reported in (*11*). The present measurements were performed in thicker samples (0.7–0.8 mm for our ACC runs compared with 0.13 mm samples in (*11*)), that were placed in cells with non-treated surfaces.

Afterwards, ASC experiments were performed for all samples A, B and C. Detailed information about the type of the run (heating or cooling), the temperature range and the average scanning rate is shown for all samples in Table 1. Figure 2 is a common plot of the (effective) C_p curves in the vicinity of the I–SmA transition. The heating runs are presented in Figure 2(a) and the cooling runs in Figure 2(b). We observe that, in the case of sample A, the transition temperature is observed at slightly higher values compared to samples B and C, which roughly coincide. The transition temperatures between the same sample's heating and cooling were almost the same and the slight hysteresis that was observed is typical for first-order transitions. The phase-coexistence range is around 200 mK, with small variations related either to the sample or to the scanning rate. A blow up of the area close to the background is shown in Figure 3, only for heating and cooling of sample A, where the abrupt evolution of the C_p values is clearly displayed. In such a plot it is easier to distinguish the exact temperature values where the heat capacity starts to evolve drastically. The extremely high values of C_p and the lack of substantial pretransitional wings reveal the signature of a strongly first-order I–SmA phase transition. One should realise that the (effective) heat capacity values around 2×10^5 J kg^{-1} K^{-1} (or 70 kJ mol^{-1} K^{-1}) are almost 100 times larger than the normal values around 2500 J kg^{-1} K^{-1} (or 0.9 kJ mol^{-1} K^{-1}), well in the I phase. No additional anomaly was observed in the vicinity of the I–SmA transition, apart from a slight change in the background values occurring only for the sample A. This change, which can be described as a very small and smeared anomaly, is observed in ASC runs closer to the I–SmA anomaly (about 0.3 K below), compared with the ACC runs. Additional observations under microscope of samples B and C did not reveal anything unusual for these two samples

Table 1. ASC runs performed for the samples A (Merck), B (BDH) and C (Likchem).

Sample	Type of run	Temperature range (*K*)	Rate[a] (K h^{-1})
A	Cooling	335–309	0.26
A	Heating	323–334	0.37
B	Cooling	336–315	0.14
B	Heating	308–338	0.43
C	Cooling	335–310	0.16
C	Heating	326–334	0.36
C	Heating	303–323	0.27

[a]This is an average value. In the phase coexistence range the rate is almost one order of magnitude slower.

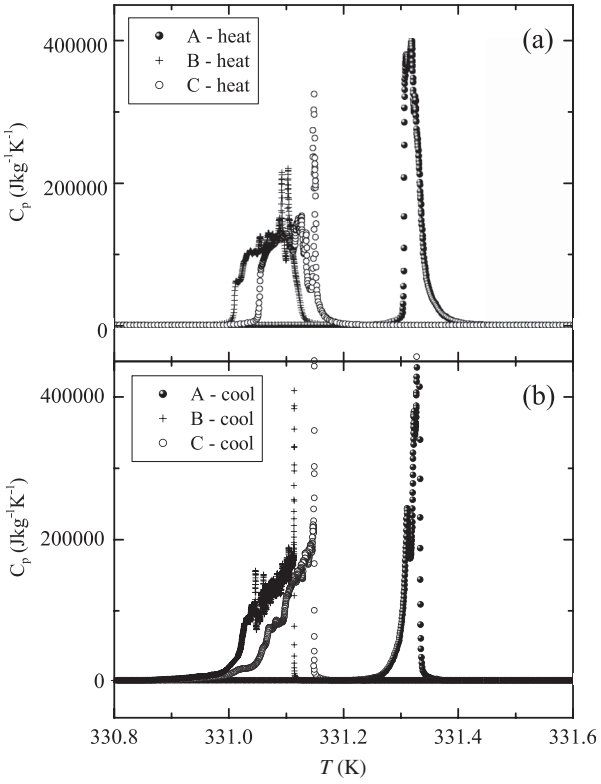

Figure 2. The $C_p(T)$ profiles in the vicinity of the I–SmA phase transition for the samples A, B and C, obtained via ASC. The heating runs are plotted in (a) and the cooling runs are plotted in (b). Solid circle, cross and open circle symbols stand for samples A, B and C, respectively.

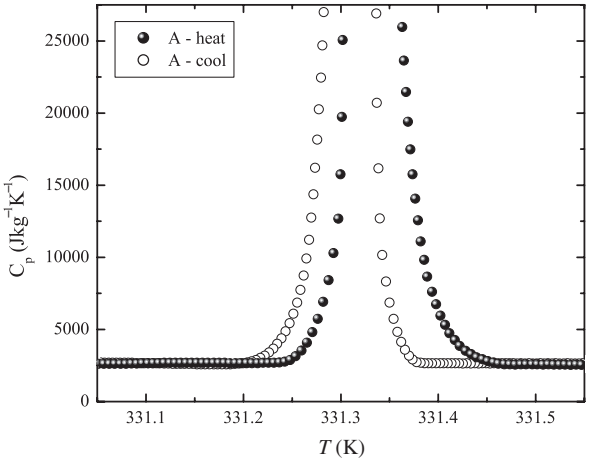

Figure 3. The $C_p(T)$ profiles of sample A are shown for heating (solid circles) and cooling (open circles). The y-axis scale is limited close to the background heat capacity, in order to clearly exhibit the points where C_p rises steeply and identify the I–SmA coexistence range.

in the temperature range of the SmA side close to the transition.

In Figure 4, the enthalpy change H in the vicinity of the I–SmA transition is shown for all runs of the samples A, B and C. The heating runs are plotted in Figure 4(a) and the cooling runs are plotted in Figure 4(b). A linear background has been subtracted from the raw data for display reasons. The density of points that we obtain via ASC is much larger than represented in this graph, but many points have been omitted for clarity. The agreement among sequential heating and cooling runs as well as between different samples is excellent, yielding a latent heat $L = 12.1 \pm 0.3$ J g^{-1}. We point out that in the case of two contiguous but still distinct phase transitions (e.g. I–N and then N–SmA) one should see two enthalpy steps (one for each transition) separated by a small temperature range with a nearly flat enthalpy behaviour. This is not the case here for any of the samples, pointing out the occurrence of only one phase transition, i.e. I–SmA.

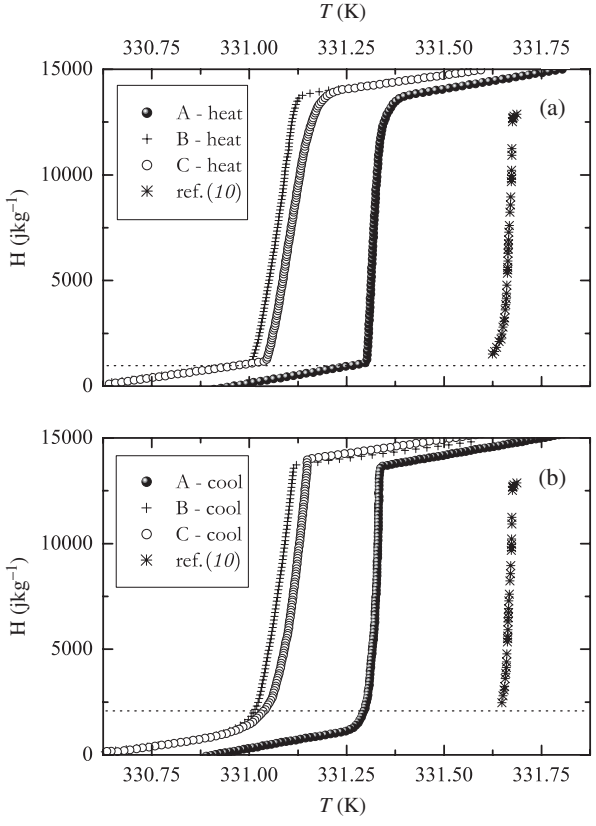

Figure 4. (a) The enthalpy changes observed in the vicinity of the I–SmA transition for all the heating runs of samples A, B and C (denoted by solid circle, cross and open circle symbols, respectively). (b) The enthalpy changes for the cooling runs. In both parts (a) and (b), an approximate enthalpy curve derived from the data of (*10*) is also plotted with our measurements, showing good agreement.

Additional polarising microscope observations of sample A did not reveal any nematic texture.

In Figure 4(a) and (b), the enthalpy curve generated from the data of (*10*) has been plotted with our results. The $C_p(T)$ data for 12CB of Buleiko and Voronov (*10*) have been read using the WinDig software. Afterwards, by using simple algebraic operations for pairs of vicinal points we estimated the enthalpy change corresponding to their $C_p(T)$ profile obtained with step adiabatic calorimetry. For each pair of vicinal points (C_{pi-1}, T_{i-1}) and (C_{pi}, T_i), one can define an enthalpy value using the very simplified formula $\Delta H_i = (T_i - T_{i-1})(C_{pi} + C_{pi-1})/2$. An enthalpy versus temperature curve $H_k(T_k)$ can be derived using the relation $H_k(T_k) = \Sigma\Delta H_i$, where $i = 1,\ldots, k$ and T_k is chosen in the middle of each temperature interval, namely $T_k = (T_i + T_{i-1})/2$. This procedure is not very precise, and it only aims to produce a curve as for comparison and not for the determination of the latent heat as such. For the latent heat one should refer to the exact value reported in (*10*), which is $L = 1.592RT$ (no error given). By substituting the values $R = 8.3145$ J K^{-1} mol^{-1}, $T = 331.67$ K and taking into consideration that 1 mol$_{(12CB)}$ = 347.536 g, one finds that $L = 12.63$ J g^{-1}, which is very close to the value we have obtained in this work.

When blowing up the data of the coexistence region, it seems that various small spikes are superimposed onto the heat capacity anomaly. These spikes should not be misinterpreted as additional phase transitions. In this out-of-equilibrium state, the conversion rate between the two phases is not constant, resulting in the appearance of these spikes when the conversion is faster. The C_p in this region has already jumped to values that are 50–100 times higher than the background values. To better demonstrate this, in Figure 5 we created a plot based on one of our runs and the step adiabatic calorimetry data of (*10*), in the units of that work. The run chosen for the comparison is the cooling of sample A.

By examining Figure 5 and comparing the peak of sample A with the its respective peak in Figure 2 and (even better) in Figure 3, one may notice the significant difference in the depiction due to the units and scale. Based on that, we arrive at the conclusion that the areas which seem like pretransitional wings in Figure 5 correspond to already abnormally high C_p values and, thus, they belong to the I–SmA coexistence region. It is only the choice of units and scale that does not allow the proper display of the steepness of the transition in the case of (*10*). An advantage of performing the ASC measurements in a scanning mode (instead of steps) is that we obtain a significantly larger number of points in the coexistence region. As a consequence, the phase-coexistence region and the

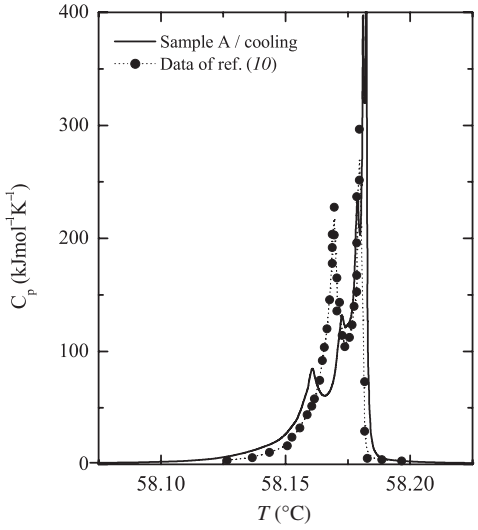

Figure 5. A common plot of $C_p(T)$ profiles for the ASC cooling run of sample A and the sample of (*10*). The aim of this plot is to demonstrate the resultant difference in the shape of the figures when the units of (*10*) are used. The abrupt evolution of heat capacity at the beginning of the two-phase region cannot be observed, and the spikes occurring at already extremely high C_p values may be misinterpreted as separate phase transitions.

shape of the anomaly can be determined more accurately.

In order to eliminate any remaining doubts about the sole appearance of the I–SmA phase transition (and not a sequence of I–N and N–SmA), we performed additional extremely slow heating and cooling runs on sample C. The features of these runs are reported in Table 2. In both cases the scanning rate in the phase-coexistence region is of the order of 10 mK h^{-1}. The $H(T)$ and the effective $C_p(T)$ profiles are shown in Figure 6(a) and (b), respectively. By assuming that a N phase exists, we should clearly see the two transitions, i.e. I–N and N–SmA, in the extremely slow runs. In addition, the two separate peaks should be visible upon both heating and cooling. In contrast, one single transition occurs here, from the I to the SmA phase. When changing the temperature so slowly, the conversion rate is more constant and the spikes are not prominent, allowing a more precise representation of the shape of the anomaly. The latent heat can now be determined with better accuracy compared with the faster runs (reported in Table 1) and it is $L = 12.24 \pm 0.08$ J g^{-1}.

Table 2. Very slow ASC runs performed for the sample C in the vicinity of the I–SmA phase transition.

Type of run	Temperature range (*K*)	Rate[a] (K h^{-1})	Rate[b] (K h^{-1})
Heating	331.6–334.1	0.05	0.009
Cooling	333.9–331.9	0.07	0.013

[a]The average rate in the total temperature range.
[b]The average rate in the coexistence region.

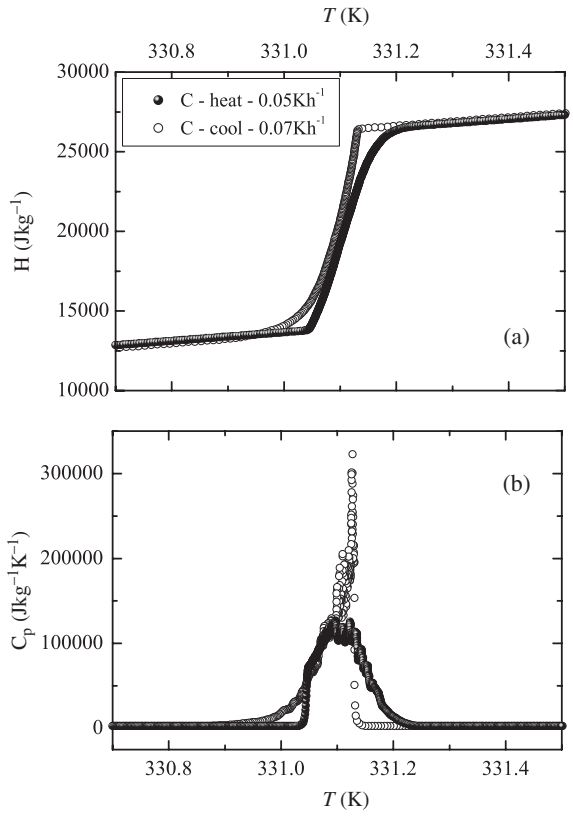

Figure 6. (a) The $H(T)$ profiles of the slow heating (solid circles) and cooling (open circles) run are plotted in the vicinity of the I–SmA transition. (b) The $C_p(T)$ profiles are shown with the same symbols. Since a massive number of points were collected, many of them have been omitted for display reasons.

The liquid crystal 12CB also undergoes a smectic A to crystal transition (SmA–Cr). This transition is well known to be strongly first-order and some DSC studies have already reported the enthalpy changes involved in it (*3, 6*). We performed ASC measurements also in the vicinity of the SmA–Cr transition, in order to accurately determine the latent heat L. The results of two heating runs, corresponding to samples B and C, were analysed for this reason. It is noteworthy that in some of the cooling runs the SmA–Cr transition was absent, because of the supercooling of the sample, often observed in nCBs. However, after leaving the sample for more than 24 hours at room temperature and then heating up we were able to trace its thermal signature. The $C_p(T)$ and the $H(T)$ profiles of the SmA–Cr transition of samples C and B are plotted in Figure 7(a) and (b), respectively. The latent heat

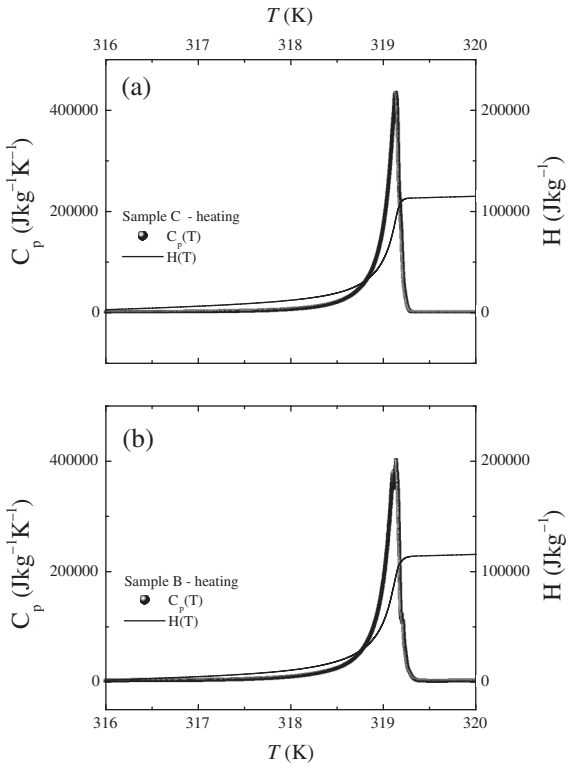

Figure 7. The $H(T)$ and $C_p(T)$ profiles in the vicinity of the SmA–Cr transition for (a) sample C and (b) sample B. In both parts the solid symbols represent the $C_p(T)$ curve and the lines the $H(T)$. Note that the units of C_p are shown on the left y-axis and those of H on the right y-axis.

determined from both runs is identical and the value $L = 102.5 \pm 1.1$ J g^{-1} is similar to the previous estimations based on DSC thermographs (*3, 6*).

We should note here that, in spite of the strongly first-order character of this transition, the $C_p(T)$ and the $H(T)$ profiles are not exactly as expected. On the side of the Cr phase, the $C_p(T)$ profile does not evolve very steeply and the $H(T)$ exhibits substantial rounding. Similar pretransitional effects, in the vicinity of strongly first-order transitions, have been observed in previous high-resolution calorimetric studies of the liquid crystals butyloxybezylidene–octylaniline (*17*) and octylcyanobiphenyl (*15*). They are attributed to the premelting of the hydrocarbon tails in the Cr phase, upon increasing the temperature, and the gradual loss of the orientational order around the chain axis.

4. Conclusions

We have carefully re-examined the phase transition sequence of 12CB by means of high-resolution calorimetry (ASC and ACC) and supplementary optical measurements. The findings of this work show that there is no N phase for 12CB. The spikes that are randomly superimposed on $C_p(T)$ in the coexistence range can be attributed to the non-constant rate of conversion between the coexisting I and SmA phases and not in a phase sequence I–N–SmA. They are dependent on the scanning rate and the type of run and they are diminished in the case of very slow cooling or heating. Concerning the N phase reported for the 12CB trapped in a glass matrix (*10*), this might have been induced by the confinement. However, no indication for a nematic phase in 12CB was found by Iannacchione *et al.* in very thin ac calorimetric cells with different surface coatings or in anopores with different surface agents (*11, 12*). On the other hand, it has been shown recently that in case of 8CB confined to controlled pore glasses the nematic phase becomes increasingly stabilised with decreasing matrix pore diameter, i.e. the nematic range increases with decreasing pore size (*14*). Thus, confinement effects might need further study.

Based on the results presented in this study, we arrive at the conclusion that the liquid crystal 12CB exhibits solely two strongly first-order transitions, namely the I–SmA and the SmA–Cr. Our high-resolution calorimetric measurements yield $L = 12.24 \pm 0.08$ J g^{-1} for the I–SmA and $L = 102.5 \pm 1.1$ J g^{-1} for the SmA–Cr phase transition. It should also be noted that, because of the substantial latent heat of the I–SmA transition, the fluctuations-induced pretransitional heat capacity increases in the SmA and I phase are small.

Acknowledgements

GC acknowledges the Research Council of K. U. Leuven for awarding a postdoctoral fellowship and J. Leys for valuable suggestions during the preparation of the manuscript.

References

(1) Gray, G.W.; Harrison, K.J.; Nash, J.A. *Electron. Lett*. **1973**, *9*, 130–131.
(2) Ashford, A.; Constant, J.; Kirton, J.; Raynes, E.P. *Electron. Lett*. **1973**, *9*, 118–120.
(3) Coles, H.J.; Strazielle, C. *Mol. Cryst. Liq. Cryst*. **1979**, *55*, 237–250.
(4) Marynissen, H.; Thoen, J.; Van Dael, W. *Mol. Cryst. Liq. Cryst*. **1983**, *97*, 149–161.
(5) Thoen, J.; Menu, G. *Mol. Cryst. Liq. Cryst*. **1983**, *97*, 163–176.
(6) Oweimreen, G.A.; Morsy, M.A. *Thermochim. Acta* **2000**, *346*, 37–47.
(7) Drozd-Rzoska, A.; Rzoska, S.J.; Ziolo, *J. Phys. Rev. E* **2000**, *61*, 5349–5354.
(8) Urban, S.; Würflinger, A; Gestblom, B.; Dabrowski, R.; Przedmojski, *J. Liq. Cryst*. **2003**, *30*, 305–311.

(9) Thoen, *J. Int. J. Mod. Phys. B* **1995**, *9*, 2157–2218.
(10) Buleiko, V.M.; Voronov, V.P. *Supramolecular Sci.* **1997**, *4*, 235–240.
(11) Iannacchione, G.S.; Strigazzi, A.; Finotello, D. *Liq. Cryst*. **1993**, *14*, 1153.
(12) Iannacchione, G.S.; Mang, J.T.; Kumar, S.; Finotello, D. *Phys. Rev. Lett*. **1994**, *73*, 2708–2711.
(13) Yao, H.; Ema, K.; Garland, C.W. *Rev. Sci. Instrum.* **1998**, *69*, 172–178.
(14) Kutnjak, Z.; Kralj, S.; Lahajnar, G.; Žumer, *S. Phys. Rev. E* **2003**, *68*, 021705.
(15) Thoen, J.; Marynissen, H.; Van Dael, W. *Phys. Rev. A* **1982**, *26*, 2886–2905.
(16) Thoen, J. In *Handbook of Liquid Crystals*; Demus, D., Goodby, J., Gray, G.W., Spiess, H.W., Vill, V., Eds.; Wiley-VCH: Weinheim, 1999; Chapter IV.
(17) Lushington, K.J.; Kasting, G.B.; Garland, C.W. *J. Phys. (Paris) Lett*. **1980**, *41*, L419–L422.